The high-pressure behaviour of Ba-doped $Na_{1/2}Bi_{1/2}TiO_3$ investigated by Raman spectroscopy

2005 J. Phys.: Condens. Matter 17 6587

(http://iopscience.iop.org/0953-8984/17/41/027)

INSTITUTE OF PHYSICS PUBLISHING JOURNAL OF PHYSICS: CONDENSED MATTER

J. Phys.: Condens. Matter **17** (2005) 6587–6597 doi:10.1088/0953-8984/17/41/027

The high-pressure behaviour of Ba-doped $Na_{1/2}Bi_{1/2}TiO_3$ investigated by Raman spectroscopy

S Trujillo[1], J Kreisel[1,4], Q Jiang[2], J H Smith[2], P A Thomas[2], P Bouvier[3] and F Weiss[1]

[1] Laboratoire des Matériaux et du Génie Physique (CNRS), ENS de Physique de Grenoble, BP 46, 38402 St Martin d'Hères, France
[2] Department of Physics, University of Warwick, Coventry CV4 7AL, UK
[3] Laboratoire d'Electrochimie et de Physicochimie des Matériaux et des Interfaces (CNRS), ENSEEG, BP 75, 38401 St Martin d'Hères Cedex, France

E-mail: jens.kreisel@inpg.fr

Received 8 July 2005, in final form 31 August 2005
Published 30 September 2005
Online at stacks.iop.org/JPhysCM/17/6587

Abstract

We report high-pressure Raman measurements up to 20.2 GPa on the perovskite-type oxide $(Na_{1/2}Bi_{1/2})_{0.89}Ba_{0.11}TiO_3$ (NBT–$BT_{0.11}$), which is of interest as a potential lead-free piezoelectric material. Distinct changes of the Raman spectra with increasing pressure illustrate that NBT–$BT_{0.11}$ shows at least two phase transitions. First, the application of low pressure progressively reduces the tetragonal signature in NBT–$BT_{0.11}$ and leads at around 1.8 GPa to a Raman spectrum reminiscent of rhombohedral NBT. Second, with further increase of pressure, the pressure-dependent behaviour of NBT–$BT_{0.11}$ resembles that of NBT and transforms to a non-cubic high-pressure structure at around 9 GPa. These observations suggest that a progressive substitution of Na^+/Bi^{3+} by Ba^{2+} pushes the pressure-induced structural instabilities of NBT towards higher pressure, corresponding to a Ba^{2+}-induced negative (tensile) pressure within the structure.

(Some figures in this article are in colour only in the electronic version)

1. Introduction

Solid solutions among ABO_3 perovskite-type oxides are well known for exhibiting a wide range of dielectric properties. One of the best known and most studied examples is the piezoelectric solid solution between $PbZrO_3$ and $PbTiO_3$, lead zirconate titanate (PZT). Recently, solid solutions between relaxor ferroelectrics (relaxors) and classical ferroelectrics have attracted an enormous interest because of the discovery [1, 2] of ultra-high strain and remarkable piezoelectric properties in single crystals such as $PbZn_{1/3}Nb_{2/3}O_3$–$PbTiO_3$ (PZN–PT) and

[4] Author to whom any correspondence should be addressed.

$PbMg_{1/3}Nb_{2/3}O_3$–$PbTiO_3$ (PMN–PT). Although such lead-containing relaxors are attractive for their outstanding properties, the toxicity of the lead-based components has caused an increasing interest in more environmentally friendly ferroelectric materials.

Most lead-free relaxors such as $BaTi_{1-x}Zr_xO_3$ (BTZ) or similar $BaTiO_3$-based materials are interesting from a fundamental point of view but do not yet offer the outstanding piezoelectric properties required for devices [3–5]. One of the very few valuable lead-free alternatives is the $Na_{1/2}Bi_{1/2}TiO_3$-based piezoelectric, which has been reported to offer exceptionally high strain when the A-site is slightly substituted by Ba^{2+} [6, 7]. Ba-doped crystals of tetragonal symmetry are reported to exhibit a free strain as large as 0.85% together with a low-field piezoelectric coefficient, $d_{33} \approx 500$ pC N^{-1} [6].

The $(1 - x)Na_{1/2}Bi_{1/2}TiO_3$–$xBaTiO_3$ (NBT–BT_x) solid solution shows structural similarities with both the PZT and PZN–PT systems. Under ambient conditions, all of these three solid solutions possess the common property that one end member is of rhombohedral symmetry while the other end member is of tetragonal $P4mm$ symmetry. The largest piezoelectric properties are observed close to the morphotropic phase boundary (MPB) composition in each system. The crystal structure at the MPB composition has monoclinic (PZT) or orthorhombic (PZN) symmetry and provides a structural bridge between the ferroelectric rhombohedral and tetragonal phases, each with their different orientation of the spontaneous polarization and cation displacements [8–10]. For NBT–BT_x the phase boundary is situated around $x \approx 0.07$ but the symmetry has yet to be determined [6, 11]. There is also still some controversy over the nature of the phase transition sequence and electric order of the phases with temperature, as for the end member $Na_{0.5}Bi_{0.5}TiO_3$ itself. In particular, the ferroelectric or anti-ferroelectric nature of the high-temperature tetragonal phase both in NBT and its solid solution with BT remains controversial, with Jones and Thomas [12, 13] suggesting, from combined neutron diffraction and second-harmonic generation measurements, that the tetragonal modification is a polar phase, and other workers [6] preferring an anti-ferroelectric assignment from hysteresis loop tracing measurements. A similar controversy exists concerning the nature of the phases in NBT–BT [11, 14].

In advancing the understanding of lead-containing piezoelectric materials, much progress has been made through temperature-dependent and/or variable chemical composition investigations (review in [10] and references cited therein). However, our current knowledge of the effect of the external parameter pressure on relaxor-based systems is relatively limited and was for a long time restricted to the low-pressure regime ($p < 1$ GPa) [15, 16]. It is only recently that investigations of relaxors have been extended to high pressure ($p > 1$ GPa), where studies have revealed that both the local and average crystallographic structures of relaxors are strongly influenced by pressure [17–22]. This suggests that intrinsic instabilities towards pressure play an important role in the observed and as yet unexplained reduction of dielectric properties in thin films of relaxors. In our high-pressure Raman investigation [22] of the relaxor-based material PMN–PT a partial x–p phase diagram was established, which illustrates that the chemical substitution of Mg^{2+}/Nb^{5+} on the B-site by Ti^{4+} leads to an important change of the pressure instabilities compared with PMN itself. In particular, this investigation suggested that PMN–PT thin films are more likely to maintain their structure against compressive strain when the Ti-content is high. However, very little is currently known about the impact of chemical substitution of the A-site on the pressure instabilities in relaxors or relaxor-related materials.

In this paper, we present the results of a study using high-pressure Raman scattering of a promising lead-free piezoelectric $Na_{1/2}Bi_{1/2}TiO_3$–$BaTiO_3$ in the application relevant regime, i.e. a tetragonal NBT–BT_x composition having $x = 0.11$ which is near the morphotropic phase boundary.

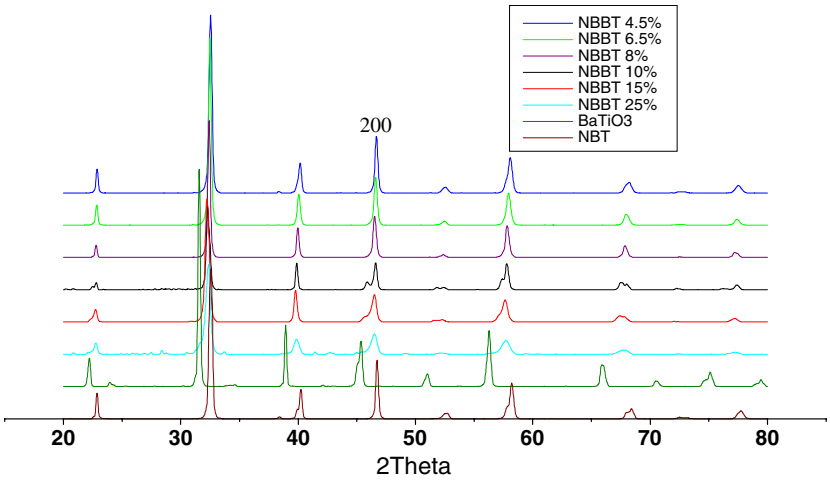

Figure 1. X-ray powder diffraction patterns of NBT–BT crystals showing tetragonal splitting of the 200 reflection for $x = 0.1$ and 0.15 nominal compositions, which correspond to ceramic compositions $x = 0.08(1)$ and 0.11(1), respectively (see figure 2).

2. Experimental details

NBT–BT_x crystals were grown via spontaneous flux crystallization in closed platinum crucibles under an air atmosphere. The starting materials consisted of reagent grade metal oxide or carbonate powders (99.9% purity) whereof stoichiometric amounts were weighed and thoroughly mixed. The ground powders were then calcined in closed platinum crucibles, re-ground and calcined again under identical conditions. Powder samples were then obtained by grinding as-grown crystals.

Depolarized Raman spectra of an NBT–$BT_{0.11}$ powder sample were recorded in back-scattering geometry with a T64000 Jobin-Yvon spectrometer using an Ar^+ ion laser (514.53 nm) as excitation line. High-pressure experiments up to 20 GPa were performed on the 300 K isotherm on powder samples which were placed in a chamber (diameter of 200 μm) of a diamond anvil cell using a 4:1 methanol–ethanol-mixture as a pressure-transmitting medium. The pressure was measured using the ruby fluorescence method [23]. Raman spectra after pressure release are identical to the initial spectra, attesting the reversibility of pressure-induced changes. An important Rayleigh scattering inhibits the access to the low-wavenumber region, which might indicate the presence of some defects such as local oxygen vacancies.

3. Results

3.1. X-ray diffraction

The x-ray diffraction data yielded by ground single crystals (figure 1) demonstrate a clear splitting of the 200 peak for the nominal 10% $BaTiO_3$ composition and for the nominal 15% $BaTiO_3$ composition. These splittings are consistent with the expected change in symmetry from rhombohedral to tetragonal with increasing $BaTiO_3$ content. The pseudocubic lattice parameter as a function of x derived from these data and the equivalent information for the ceramics (figure 2) show that the crystals are systematically low in Ba compared with the starting composition, in agreement with the findings of [7] for growth from the flux. Thus, the nominal 10% and 15% $BaTiO_3$ single-crystal compositions are actually closer to $x = 0.075$ and

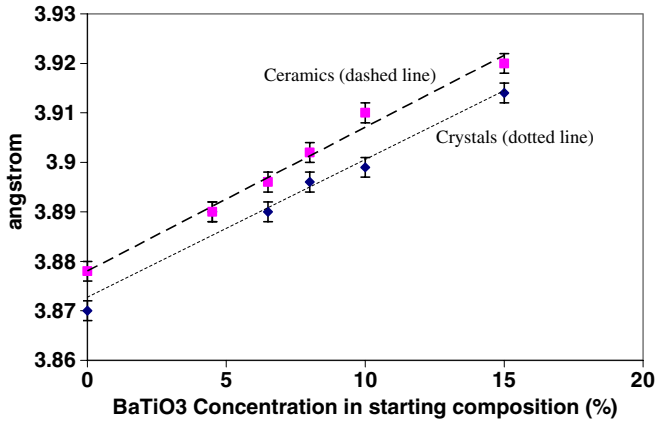

Figure 2. Pseudo-cubic lattice parameters derived from x-ray data for NBT–BT single crystals (as a function of nominal starting composition) and ceramics. The lattice parameter for crystals of nominal starting composition $x = 0.15$ is seen to correspond to the ceramic composition $x = 0.11(1)$.

0.115 (NBT–$BT_{0.11}$), respectively. The (3/2 1/2 1/2) $a^-a^-a^-$ tilt [24] peak that is observed in the room-temperature powder diffraction pattern of NBT itself is consistent with space group $R3c$ [13, 25] but diminishes successively in intensity for ceramics and crystal compositions with $x = 0.045$ and 0.065. This tilt peak is no longer visible for $x \geqslant 0.08$. The diffraction patterns from the tetragonal compositions with $x \geqslant 0.1$ display no visible super-lattice peaks and are consistent with $P4mm$ symmetry. Powder samples were obtained from ground as-grown single crystals. For the following Raman study we have chosen the NBT–$BT_{0.11}$ sample which is of tetragonal symmetry and thus slightly above the rhombohedral–tetragonal phase boundary (around $x \approx 0.08$) but not within. Note that such a chemical substitution above the morphotropic phase boundary leads to a slight reduction of the outstanding properties but has the important technological advantage of avoiding chemical/structural fluctuation problems (similarly to what is applied to commercially used PMN–PT crystals).

3.2. Raman spectrum at ambient pressure

Figure 3 presents the Raman spectrum of NBT–$BT_{0.11}$ together, for comparison, with Raman spectra of NBT–$BT_{0.045}$, the end members $Na_{1/2}Bi_{1/2}TiO_3$, $BaTiO_3$ and those of the related materials $K_{1/2}Bi_{1/2}TiO_3$ and $Na_{1/2}Bi_{1/2}TiO_3$–$K_{1/2}Bi_{1/2}TiO_3$.

The spectrum of NBT–$BT_{0.11}$ is similar to that of $Na_{1/2}Bi_{1/2}TiO_3$ but there are the following differences.

(i) The NBT band at about 135 cm^{-1} decreases in intensity and displays a shift to low wavenumbers for NBT–$BT_{0.11}$.
(ii) The broad and characteristic band centred for NBT around 260 cm^{-1} presents at 300 cm^{-1} a marked high-wavenumber shoulder for NBT–$BT_{0.11}$.
(iii) The overlapping bands around 400–650 cm^{-1} for NBT are split into at least two distinct bands for NBT–$BT_{0.11}$.

These three spectral changes are consistent with a compositionally driven structural phase transition, from rhombohedral symmetry on average to tetragonal, occurring between NBT and NBT–$BT_{0.11}$. Let us parenthesize that the Raman spectrum of NBT–$BT_{0.045}$ is still very similar

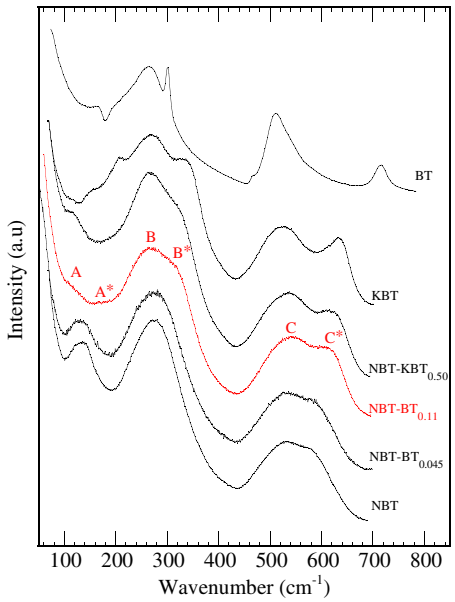

Figure 3. The 300 K Raman spectrum of $(Na_{1/2}Bi_{1/2})_{0.89}Ba_{0.11}TiO_3$ (NBT–$BT_{0.11}$), in red (third from the bottom), in comparison to those of the end members $Na_{1/2}Bi_{1/2}TiO_3$ (NBT), $BaTiO_3$ (BT) and of the related materials $K_{1/2}Bi_{1/2}TiO_3$ (KBT) and $(Na_{0.5}K_{0.5})_{1/2}Bi_{1/2}TiO_3$ (NBT–$KBT_{0.5}$).

to that of pure NBT, which suggests a rhombohedral structure, and that the rhombohedral-to-tetragonal phase transition occurs for $x > 0.045$. It will be the scope of section 3.3.3 to follow the new tetragonal-characteristic spectral features as a function of pressure.

Considering now the other spectra in figure 3, we note that the Raman spectrum of NBT–$BT_{0.11}$ is reminiscent of the Raman signature that has been reported earlier [26] for the $x = 0.20$ substitution in the NBT-related $(1-x)Na_{1/2}Bi_{1/2}TiO_3$–$xK_{1/2}Bi_{1/2}TiO_3$ (NBT–KBT_x) solid solution. Such a spectral similarity between NBT–BT and NBT–KBT is initially surprising, since the Raman signatures of the end members BT and KBT are very different (figure 3). However, it should be noted that the Raman spectra of relaxors generally show only slight (if any) spectral changes upon chemical substitution but tend to be dominated by a signal characteristic of the general disorder in the system. For example, the Raman signature of PMN–PT hardly changes in the $0 \leqslant x \leqslant 0.4$ substitution regime, although its average structure undergoes a cubic $\rightarrow$ rhombohedral $\rightarrow$ monoclinic $\rightarrow$ tetragonal phase sequence with increasing x [27, 28]. The similarities observed for NBT–BT and NBT–KBT are consistent with the spectrum being dominated by disorder (just as for NBT itself) coupled with the introduction of tetragonality by the BT or KBT doping, respectively.

3.3. Raman spectrum at high pressure

Figure 4 presents the overall evolution of the Raman spectra for NBT–$BT_{0.11}$ as a function of the applied hydrostatic pressure up to 20.2 GPa. The notations used throughout the text for the different bands in the NBT–$BT_{0.11}$ are given in figure 3.

3.3.1. Low-wavenumber region (100-to-200 cm^{-1}). The spectrum of NBT–$BT_{0.11}$, just as observed for NBT powder samples, presents an important central scattering component, which partly masks two underlying bands: band A and band A*. Bands in this region have been

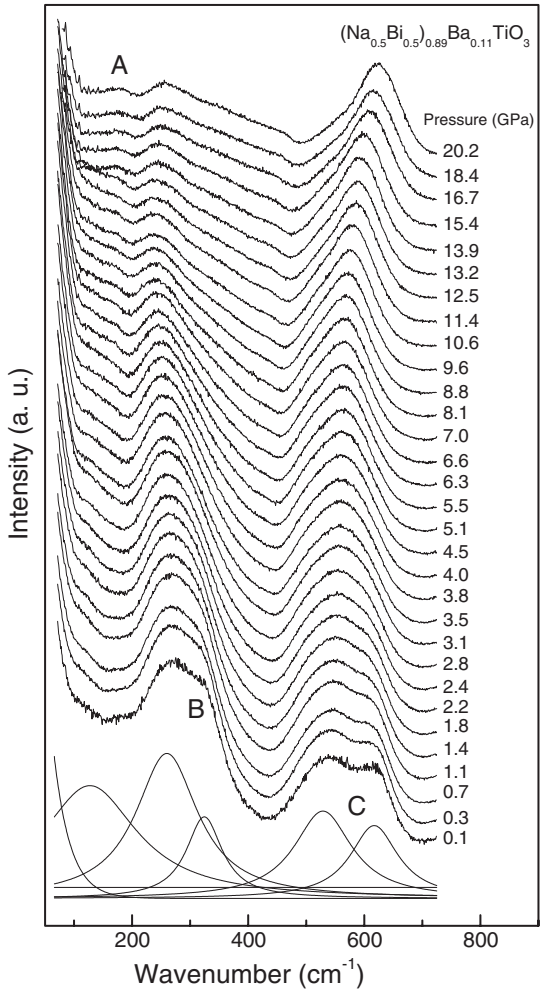

Figure 4. Pressure-dependent Raman scattering of $(Na_{1/2}Bi_{1/2})_{0.89}Ba_{0.11}TiO_3$ (NBT–$BT_{0.11}$). The important pressure-induced modifications of the spectral signature point to a structural rearrangement under high pressure. For illustration, a spectral deconvolution of the ambient-pressure data is also shown.

assigned to A-cation vibrations and are expected to be sensitive towards phase transitions in which the A-site symmetry changes. Unfortunately, a quantitative analysis of the low-wavenumber region in terms of a spectral deconvolution is not viable due to the strong central scattering wing. However, a qualitative inspection of the pressure-dependent spectra shows a low-wavenumber shift of band A* up to say 2 GPa from where on a single band A shifts to higher wavenumbers. At higher pressure B and A becomes a clearly distinguishable spectral component.

3.3.2. Mid-wavenumber region (200-to-450 cm^{-1}). The broad and intense feature centred around 280 cm^{-1} is the dominant feature in the NBT–$BT_{0.11}$ Raman spectrum at ambient conditions. The broad feature is composed of the NBT-type band B and the Ba-induced feature B*. Three main pressure-induced changes can be discerned.

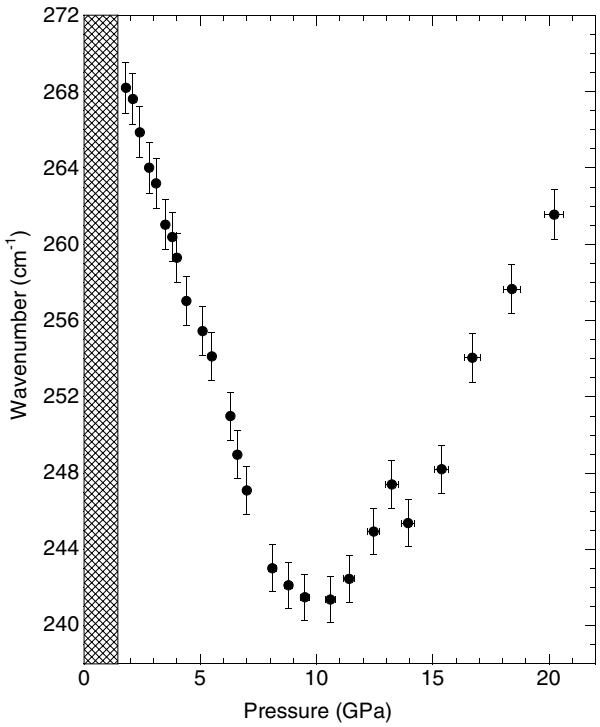

Figure 5. Pressure-dependent evolution, from 1.8 GPa onwards, of the position in wavenumber for the initially dominant band around 260 cm^{-1}. The anomaly in the 9–10 GPa range indicates a phase transition. The hatched zone below corresponds to the low-pressure phase, which is characterized by a supplementary high-wavenumber shoulder that shifts gradually to the 260 cm^{-1} band up to 1.8 GPa where the two bands merge. Although the latter behaviour is qualitatively easily observed, the spectral deconvolution of this band coalescence was not stable due to the strong central Raleigh scattering and the high-wavenumber wing of the band at 260 cm^{-1}.

(i) First, band B* shows a low-wavenumber shift towards band B and from $p = 1.8$ GPa onwards bands B and B* are no longer distinguishable. Although the new merged feature can still be deconvoluted with two components we have chosen to fit this region with a single large band to allow a better analysis of the behaviour above for $p > 1.8$ GPa.

(ii) The broad feature shows up to $p \approx 10$ GPa a low-wavenumber shift, where a discontinuity is observed, after which band B shifts to higher wavenumbers. Figure 5 shows the pressure-dependent evolution of wavenumber for band B as deduced from a spectral deconvolution.

(iii) While the intensity of the high-wavenumber region remains almost unchanged with increasing pressure, the mid-wavenumber feature decrease dramatically in intensity. In order to emphasize this spectral feature figure 6 presents the pressure-dependent spectra of NBT–$BT_{0.11}$ directly superimposed and normalized to the high-wavenumber region. Note that the illustrated pressure behaviour is unusual and has only been observed for the relaxors NBT and PMN [17, 18] or the relaxor-related system PMN–PT [22] but is, for instance, not observed for the piezoelectric PZT [29].

Each of the above points can be seen as a direct indication for fundamental pressure-induced changes of NBT–$BT_{0.11}$. For the understanding of the underlying structural changes it is useful to remember that this spectral region can be assigned to vibrations of A_1 symmetry dominated by TiO_6 octahedra [30]. In a general matter, it has been shown that changes

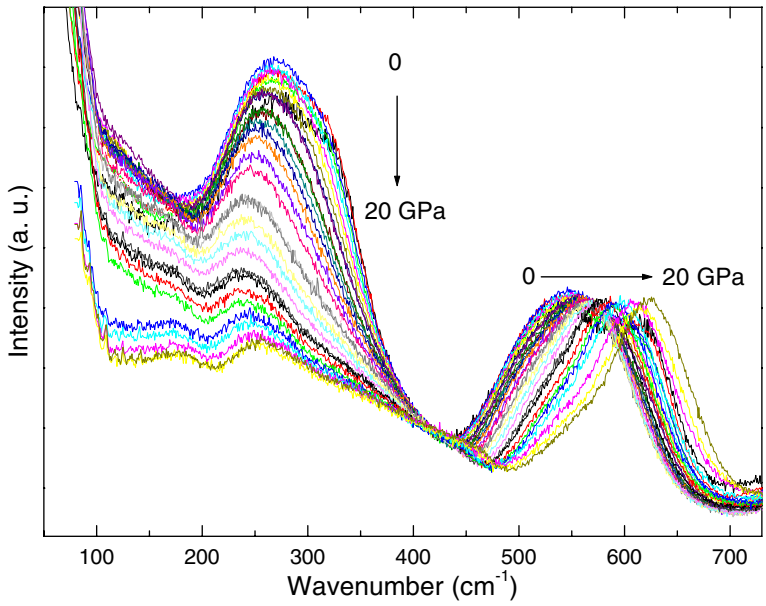

Figure 6. Representative pressure-dependent Raman spectra for $(Na_{1/2}Bi_{1/2})_{0.89}Ba_{0.11}TiO_3$, directly superimposed and normalized to the high-wavenumber bands in order to emphasize the important intensity changes in the mid-wavenumber region.

related to the polar Ti-cation displacement but also to the octahedron-tilt-related distortion lead to important changes in the mid-wavenumber region. Both its intensity evolution and its band-shift have been used to identify phase transitions in classic [31–33] and complex ferroelectrics [34–36]. In the light of the above, both the anharmonic low-wavenumber shift (figure 5) and the dramatic intensity breakdown in the mid-wavenumber region (figure 6) provide a spectral signature for a structural rearrangement which is related to changes of the TiO_6 octahedra.

3.3.3. High-wavenumber region (450-to-700 cm^{-1}). In oxides, vibrational modes at high wavenumber are dominated by vibrations involving mainly oxygen displacements and can often be interpreted in terms of polyhedron vibrations [37–39]. Although a direct vibrational signature such as soft modes is not expected at high wavenumber, this region can be instructive because any structural change should affect at least slightly the whole phonon spectrum (concept of hard-mode spectroscopy [40, 41]).

The high-wavenumber region of NBT–$BT_{0.11}$ is composed of two overlapping bands: band C and band C*. For NBT such high-wavenumber bands have been assigned to oxygen vibrations of the TiO_6 octahedra [17]. With applied pressure the overlap of the two bands increases and leads to a coalescence into a single broad band.

4. Discussion

Summarizing the above spectral analysis, we note that the pressure-dependent Raman signature presents at least two marked modifications: a first modification in the low-pressure regime (change in band A, coalescence of bands B and B*, coalescence of bands C and C*) and then a second modification in the high-pressure regime ($d\nu/dp$ slope change of band B, new

band C**). The remaining question concerns the nature of the underlying pressure-induced structural rearrangement. We should first recall that pure NBT presents a complex distortion from the cubic $Pm\bar{3}m$ prototype structure via both A- and B-cation displacements and tilted octahedra [13]. The delicate interplay of such distortions in perovskites is usually modified via external parameters like temperature or pressure as has been evidenced for NBT via x-ray and neutron diffraction [12, 13, 42, 43]. We expect a similar situation for NBT–$BT_{0.11}$ and thus the spectral changes in the different typical regions of the spectrum suggest a structural rearrangement related to the different types of distortion. Unfortunately, the breakdown of the Raman selection rules in relaxors and relaxor-related materials does not allow a straightforward interpretation of the Raman scattering in terms of symmetry (and of course even less in terms of a specific space group). Nevertheless, the discussion of the spectral analysis and the fact that Raman spectroscopy is a fingerprint technique allows drawing the following preliminary picture.

The downshift of band B* illustrates that pressure reduces considerably the initial Ba^{2+}-induced tetragonality in NBT–$BT_{0.11}$. Parallel to this evolution the split of bands C and C* decreases. Around a critical pressure of 1.8 GPa this trend leads in the mid- and high-wavenumber region to the known spectral signature of rhombohedral NBT (figure 3) which suggests that NBT–$BT_{0.11}$ then adopts a very similar or even identical distortion. With increasing pressure band B shows a considerable band softening while all the other features increase in wavenumber. This behaviour is similar to what has been observed for NBT in the low-pressure regime [17]. The band softening with pressure can be understood in terms of an anharmonic contribution and thus provides a strong indication of an approaching phase transition. Such a phase transition is then manifest by a $d\nu/dp$ slope change of band B at 10 GPa (similar to what is observed around 5 GPa for NBT). In the same pressure regime we observe the development of a new low-wavenumber shoulder C** and of a high-wavenumber wing of band B in the form of a density-of-state-like feature, which suggests a symmetry lowering as observed for NBT [17].

A remaining question concerns the structure of the high-pressure phase of NBT–$BT_{0.11}$. Perovskite-type ferroelectrics are commonly expected to become cubic at high pressure. The argument for this comes mainly from the observation that $ATiO_3$ (A = Ba and/or Pb) show pressure-induced soft modes together with an overall intensity lowering of the Raman spectrum [31–33]. Despite the fact that any first-order Raman scattering is forbidden in the $Pm\bar{3}m$ structure, Raman spectra have been observed for several cubic perovskites because of a breakdown of the Raman-scattering selection rules resulting from disorder of the Ti positions and/or the presence of ferroelectric microregions. As a consequence, even though we observe a Raman spectrum at high pressure the 'parent' cubic perovskite structure could still be a plausible candidate. However, we believe that the high-pressure Raman spectrum of NBT–$BT_{0.11}$ is too well defined for a cubic $Pm\bar{3}m$ phase. Support comes from the fact that the high-pressure signature of NBT–$BT_{0.11}$ is very similar to the spectrum observed for the high-pressure phase of NBT [17], for which x-ray and neutron diffraction have unambiguously attested a non-cubic structure [19, 42, 43]. The above is in agreement with the more recent idea that complex ferroelectrics maintain a non-cubic average structure at high pressures [17–20, 22, 44].

Resuming the above, pressure (and presumably strain in thin films) has a considerable impact on NBT–$BT_{0.11}$ and we can describe the effect of pressure on NBT–$BT_{0.11}$ in two regimes: a first in which the application of low pressure forces NBT–$BT_{0.11}$ into the NBT structure and a second in which NBT–$BT_{0.11}$ follows the pressure behaviour of NBT. As a consequence, a progressive substitution of Na^+/Bi^{3+} by Ba^{2+} pushes the pressure-induced structural instabilities of NBT towards higher pressure, just as if Ba induces a negative (tensile) pressure. Indeed, we note that the ionic radius of Ba^{2+} is about 30% larger than the ionic radii

of Na^+ and Bi^{3+}, which leads to an increase in the lattice parameter and thus a negative chemical pressure. Considering that Na/Bi–O and Ba–O involve the same chemical bonds and using the compressibility κ defined by

$$\kappa = -\frac{1}{V}\frac{\partial V}{\partial P}\bigg|_T \tag{1}$$

we can make an estimate of the Ba^{2+}-induced negative pressure. If we further assume that NBT and NBT–$BT_{0.11}$ can be described by pseudo-cubic structures with a lattice parameter a and that the unit cell volume V varies linearly with the applied hydrostatic pressure P, the compressibility in equation (2) can be described as [45]:

$$\kappa = -3\frac{\Delta a}{a}\frac{1}{\Delta P}. \tag{2}$$

Applying equation (2) with $a_{NBT} = 3.88$ Å, $a_{NBBT(11)} = 3.90$ Å and $\kappa \approx 6.3\times10^{-3}$ GPa^{-1} [45] leads to 'chemical' pressure of $\Delta P \approx -2.5$ GPa. This value is of the order of the critical pressure where NBT–$BT_{0.11}$ adopts the NBT spectral signature and thus supports the idea of a Ba^{2+}-induced negative pressure.

Acknowledgments

QJ, JHS and PAT are grateful to the Engineering and Physical Science Research Council (EPSRC, GB) for a grant that enabled this work to be pursued. ST, JK and FW acknowledge financial support from the European Network of Excellence FAME. ST is grateful to CONACYT and SEP for financial support.

References

[1] Park S E and Shrout T R 1997 *J. Appl. Phys.* **82** 1804
[2] Kobayashi T, Shimanuki S, Saitoh E and Yamashita Y 1997 *Japan. J. Appl. Phys.* **36** 6035
[3] Ravez J and Simon A 1997 *Eur. Phys. J.: Appl. Phys.* **34** 1199
[4] Rehring P W, Park S E, Trolier-McKinstry S, Messing G L, Jones B and Shrout T R 1999 *J. Appl. Phys.* **86** 1657
[5] Farhi R, Marssi M E, Simon A and Ravez J 1999 *Eur. Phys. J.* B **9** 559
[6] Chiang Y-M, Farrey G W and Soukhojak A N 1998 *Appl. Phys. Lett.* **73** 3683
[7] Sheets S A, Soukhojak A N, Ohashi N and Chiang Y M 2001 *J. Appl. Phys.* **90** 5287
[8] Noheda B, Cox D E, Shirane G, Gonzalo J A, Cross L E and Park S E 1999 *Appl. Phys. Lett.* **74** 2059
[9] Noheda B, Cox D E, Shirane G, Guo R, Jones B and Cross L E 2001 *Phys. Rev.* B **63** 014103/1
[10] Noheda B 2002 *Curr. Opin. Solid State Mater. Sci.* **6** 27
[11] Takenaka T, Maruyama K and Sakata K 1991 *Japan. J. Appl. Phys.* **30** 2236
[12] Jones G O and Thomas P A 2000 *Acta Crystallogr.* B **56** 426
[13] Jones G O and Thomas P A 2002 *Acta Crystallogr.* B **58** 168
[14] Gomah-Pettry J R, Said S, Marchet P and Mercurio J P 2004 *J. Eur. Ceram. Soc.* **24** 1165
[15] Samara G A, Venturini E L and Schmidt V H 2000 *Appl. Phys. Lett.* **76** 1327
[16] Samara G A 2000 *AIP Conf. Proc.* **535** 344
[17] Kreisel J, Glazer A M, Bouvier P and Lucazeau G 2001 *Phys. Rev.* B **63** 174106
[18] Kreisel J, Dkhil B, Bouvier P and Kiat J M 2002 *Phys. Rev.* B **65** 172101
[19] Kreisel J *et al* 2003 *Phys. Rev.* B **68** 014113
[20] Chaabane B, Kreisel J, Dkhil B, Bouvier P and Mezouar M 2003 *Phys. Rev. Lett.* **90** 257601
[21] Kreisel J, Bouvier P, Maglione M, Dkhil B and Simon A 2004 *Phys. Rev.* B **69** 092104
[22] Chaabane B, Kreisel J, Bouvier P, Lucazeau G and Dkhil B 2004 *Phys. Rev.* B **70** 134114
[23] Piermarini G J, Block S, Barnett J D and Forman R A 1975 *J. Appl. Phys.* **46** 2274
[24] Glazer A M 1972 *Acta Crystallogr.* B **28** 3384
[25] Vakhrushev S B, Kvyatkovskii B E, Malysheva R S, Okuneva N M and Syrnikov P P 1985 *Fiz. Tverd. Tela* **27** 737

[26] Kreisel J, Glazer A M, Jones G, Thomas P A, Abello L and Lucazeau G 2000 *J. Phys.: Condens. Matter* **12** 3267
[27] Idink H and White W B 1994 *J. Appl. Phys.* **76** 1789
[28] Ohwa H, Iwata M, Orihara H, Yasuda N and Ishibashi Y 2001 *J. Phys. Soc. Japan* **70** 3149
[29] Sani A, Noheda B, Kornev I A, Bellaiche L, Bouvier P and Kreisel J 2004 *Phys. Rev.* B **69** 020105
[30] Zhang M S and Scott J F 1986 *Ferroelectr. Lett.* **6** 147
[31] Sanjurjo J A, Lopez-Cruz E and Burns G 1983 *Phys. Rev.* B **28** 7260
[32] Venkateswaran U D, Naik V M and Naik R 1998 *Phys. Rev.* B **58** 14256
[33] Burns G, Sanjurjo J A and Lopez-Cruz E 1984 *Phys. Rev.* B **30** 7170
[34] Vugmeister B E, DiAntonio P and Toulouse J 1995 *Phys. Rev. Lett.* **75** 1646
[35] Toulouse J, DiAntonio P, Vugmeister B E, Wang X and Kraus L A 1992 *Phys. Rev. Lett.* **68** 232
[36] DiAntonio P, Vugmeister B E, Toulouse J and Boatner L A 1993 *Phys. Rev.* B **47** 5629
[37] Tarte P, Rulmont A, Liégeois-Duycckaerts M, Cahay R and Winand J M 1990 *Solid State Ion.* **42** 177
[38] Tarte P 1967 *Spectrochim. Acta* **A23** 2127
[39] Kreisel J, Lucazeau G and Vincent H 1998 *J. Solid State Chem.* **137** 127
[40] Bismayer U 1990 *Phase Transit.* **27** 211
[41] Salje E K H and Bismayer U 1997 *Phase Transit.* **63** 1
[42] Jones G O, Kreisel J, Jennings V, Geday M A, Thomas P A and Glazer A M 2002 *Ferroelectrics* **270** 191
[43] Thomas P A, Kreisel J, Glazer A M, Bouvier P, Jiang Q and Smith R 2005 *Z. Kristallogr.* **220** 717
[44] Kreisel J *et al* 2004 *Ferroelectrics* **302** 539
[45] Kreisel J and Glazer A M 2000 *J. Phys.: Condens. Matter* **12** 9689